Deep Learning-aided TR-UWB MIMO System

Umer Zia *Student Member IEEE*, Wei Xiang *Senior Member IEEE*, Tao Huang *Senior Member IEEE*, and I.H Naqvi *Senior Member IEEE.*

***Abstract*—This paper presents a novel deep learning-aided scheme dubbed $PR\rho$-net for improving the bit error rate (BER) of the Time Reversal (TR) Ultra-Wideband (UWB) Multiple Input Multiple Output (MIMO) system with imperfect Channel State Information (CSI). The designed system employs Frequency Division Duplexing (FDD) with explicit feedback in a scenario where the CSI is subject to estimation and quantization errors. Imperfect CSI causes a drastic increase in BER of the FDD-based TR-UWB MIMO system, and we tackle this problem by proposing a novel neural network-aided design for the conventional precoder at the transmitter and equalizer at the receiver. A closed-form expression for the initial estimation of the channel correlation is derived by utilizing transmitted data in time-varying channel conditions modeled as a Markov process. Subsequently, a neural network-aided design is proposed to improve the initial estimate of channel correlation. An adaptive pilot transmission strategy for a more efficient data transmission is proposed that uses channel correlation information. The theoretical analysis of the model under the Gaussian assumptions is presented, and the results agree with the Monte-Carlo simulations. The simulation results indicate high performance gains when the suggested neural networks are used to combat the effect of channel imperfections.**

I. Introduction

The recent advancements in wireless communication systems have resulted in a continued desire for higher and higher data rates. Ultra-Wideband (UWB) systems not only provide a higher data rate but also computes the precise location of the mobile station owing to its temporal focusing property [1], [2]. The last decade has seen widespread use of this technology in healthcare applications, wireless local area networks, and wireless personal area networks in accordance with IEEE 802.15 standard [3]. Recently, this technology has been adopted by leading manufacturers of smartphones to gain improved spatial and location awareness [4]. Moreover, novel UWB antenna designs are under rigorous investigation by researchers [5], [6].

The transmission in Ultra-Wideband has several benefits over their narrow-band counterparts. Apart from UWB spectral and regulatory advantages like ultra-large bandwidth, low interference to other wireless systems, and license-free spectrum, the UWB, in conjunction with the time-reversal (TR) technique, also offers the gains of temporal and spatial focusing [7]. The temporal focusing means that the received signal is compressed in the time domain, which diminishes the Inter Symbol Interference (ISI) to a large extent, whereas the spatial focusing property brings the two-fold advantage of secure communication and reduction in Multi-User Interference (MUI) as the received signal appears to be a noise-like signal to unintended users [8]. The availability of a very large bandwidth in UWB causes signal bandwidth to almost always exceed the coherence bandwidth of the channel resulting in frequency selective fading, which in turn makes receiver design complex. In the time-reversal communication system, by precoding transmitted signals with the complex conjugated and time-reversed channel impulse response, the need for a complex receiver can be alleviated. Note that the TR-UWB Multiple Input Multiple Output (MIMO) system does not nullify interference like conventional Space Division Multiplexing (SDM) Singular Value Decomposition (SVD) MIMO system but minimizes it; thus, a good reception needs equalization at the receiver [9]. Along with several advantages, several challenges also exist in TR-UWB MIMO systems, in particular, when it is deployed in Frequency Division Duplex (FDD) settings. In terms of precoding and beamforming, imperfect or delayed Channel State Information (CSI) severely affects the performance in FDD TR-UWB MIMO systems [10]. Traditionally, the TR-UWB MIMO beamforming assumes channel reciprocity in a Time Division Duplex (TDD) scenario; however, there has been an increasing demand for solutions for FDD systems. To the best of the authors' knowledge, there is no prior work in terms of a neural net solution in FDD based TR-UWB MIMO system. The key contributions of our research are three-fold:

1) A novel Deep Learning based architecture dubbed $PR\rho$-net is proposed to improve channel estimation at the precoder and receiver in the presence of imperfect CSI. The proposed DL-based architecture is novel in terms of imperfect CSI mitigation at precoder and equalizer simultaneously.
2) The proposed $PR\rho$-net also estimates channel correlation ρ from transmitted data symbols in a time-varying channel that follows the first-order autoregressive model. The DL-aided system brings improvements by accurately estimating the CSI at the precoder as well as the equivalent channel and ρ at the receiver.
3) Based on the receiver's knowledge of the instantaneous value of the channel correlation, we propose an adaptive pilot re-transmission scheme that can reduce the frequency of channel estimation, thereby resulting in an increase in transmission of useful user data instead of the pilot sequences. The knowledge of time-varying channel conditions aids in setting a pilot re-transmission frequency for the desired bit error rate (BER).

The rest of the paper is organized as follows. In Section II, state of the art in TR-UWB MIMO and Deep Learning techniques concerning channel estimation are presented. The TR-UWB-MIMO system model and our objective are described in Section III. Section IV investigates the $PR\rho$ neural network design for TR-UWB-MIMO systems, while simulation results are discussed in Section V. Finally, Section VI concludes the

paper.

Notation: We denote scalars, vectors, and matrices by regular letters, lowercase bold letters, and uppercase bold letters, respectively. For a matrix $\mathbf{A}$, we denote its transpose and Hermitian transpose by $\mathbf{A}^{\mathrm{T}}$ and $\mathbf{A}^{\mathrm{H}}$, respectively. An identity matrix is denoted by $\mathbf{I}$ and the expected value by $\mathbb{E}$. Matrix $\mathbf{A}$ with M rows and N columns is denoted by $\mathbf{A}_{M\times N}$.

II. Related Work

In this section, we will review the research literature on UWB MIMO systems with a focus on the TR technique, as well as recent work on deep learning with an emphasis on channel estimation and feedback methodologies.

A. UWB and MIMO

The initial work in TR-UWB MIMO practical demonstration was done by [8], [9] and [12]. In [10], a robust feedback design is proposed to mitigate the combined effect of quantization, feedback delay, and noise on the feedback channel. The investigators in [11] proposed a conventional Minimum Mean Square Error (MMSE) equalizer to minimize multi-stream interference. The investigation in [13] focused on the spatial correlation among the transmit and receive antennas with TR pre-filter and Zero Forcing (ZF) pre-equalizer utilized for interference mitigation. An ordered successive interference cancellation scheme is applied in [14] for detection in ultra-wideband MIMO communication systems with RAKE combining. In [15], [16], the authors investigated the role of MMSE successive interference cancellation with modulation schemes having high spectral efficiency. In [17], researchers presented interference-nulling time-reversal, a beamforming technique for multi-user frequency-selective indoor channels. The pre-equalizer designs to cope with multi-stream and inter-symbol interference were investigated by H. Nguyen et al. [18] and T. Wang et al. [19], respectively. In [20], the investigators explored the impact of using a single antenna to form a virtual MIMO system, while a reduction in transmit antenna for improved performance is suggested by [21]. Moreover, researchers in [22] and [23] focused on improved TR pre-filter and post-filter designs for improved transmission. Researchers in [24] investigated the performance of the time-reversal system in time-varying conditions using the first-order autoregressive model.

B. Deep Learning for Channel Estimation

In the field of deep learning, several solutions regarding MIMO inherent issues as well as channel estimation problems are proposed by researchers [25], [26]. The key works in the area of CSI feedback include [27] and [28], which explored CSI encoding and multi-resolution CSI feedback, respectively. Moreover, researchers in [29] investigated the impact of Cyclic Prefix (CP) removal and variable-length pilots in Orthogonal Frequency Division Multiplexing (OFDM) systems when deep learning is applied for channel estimation and signal detection. Similarly, in [30] a Deep Learning-based channel estimation algorithm is proposed for the scenario when channels undergo both frequency and time selective fading. In [31], the authors presented DL-based algorithm termed as ChannelNet for channel estimation by considering the time-frequency response of a fading channel as a 2D-image and further applied Convolutional Neural Network (CNN) to estimate the whole channel state. On channel prediction for FDD-based massive MIMO systems, Yang et al. [32] investigated the DL-aided uplink-to-downlink channel mapping function in the FDD scenario. In a similar investigation by Yang et al. [33], downlink CSI prediction for the users in different environments is addressed by Deep Transfer Learning (DTL). The research in [34] focuses upon DL-based optimization of feedback and precoding of multiuser massive MIMO systems. Similarly, the research in [35] investigates the use of DL techniques for joint pilot design and channel estimation in multiuser MIMO to minimize the mean square estimation error of the channel. A common issue of the FDD and UWB-based MIMO systems lies in cumbersome channel estimation and its feedback that often faces degradation due to quantization and delay. However, compared to other FDD-based MIMO systems, the UWB systems are deployed in relatively stationary channel environments and can benefit from a DL-aided design that tackles channel corruption while minimizing pilot re-transmissions. Although there is sufficient literature on precoding, equalization, and ISI mitigation, the literature still lacks a Deep Learning based system design that deals with overall CSI imperfections. Our research concentrates on the Deep Learning aided improvement of channel quality at precoder and receiver (equalizer). Furthermore, a Deep Learning assisted method of evaluating channel correlation and correlation-dependent re-transmission of pilots in TR-UWB MIMO system considering FDD scenario is also presented.

III. System Model and Problem Formulation

In this section, we will first introduce the system model. Then in subsequent subsections, we will elaborate on the system under perfect and imperfect CSI cases as well as narrate the problem addressed by our design.

A. System Overview

The block diagram of the TR-UWB MIMO system operating in FDD settings is shown in Fig. 1 (a). We assume an equal number of transmit (N_{T}) and receive antennas (N_{R}) in the system model i.e., $N_{\mathrm{T}} = N_{\mathrm{R}} = N$. The transmitted data taken from set $\{\pm 1\}$ is divided into N parallel data streams for achieving MIMO Spatial Multiplexing (SM) gain. Each data bit of these parallel streams has energy represented by $\sqrt{\mathrm{E_b}}$. The bits are then pulse shaped by the second order Gaussian mono-pulse [13] and then modulated using Binary Phase Shift Keying (BPSK) to form a signal $\mathbf{s}(t) = d\mathbf{p}(t)$, where d represents the data bit, $\mathbf{p}(t)$ is the second order Gaussian pulse given by

$$\mathbf{p}(t) = \left[1 - 4\pi\left(\frac{t - t_{\mathrm{c}}}{T_{\mathrm{p}}}\right)^2\right] \mathrm{e}^{-2\pi\left(\frac{t-t_{\mathrm{c}}}{T_{\mathrm{p}}}\right)^2} \tag{1}$$

where T_{p} is the pulse existing period and t_{c} is the time shift of the pulse. The pulse is normalized to unit energy

This article has been accepted for publication in IEEE Transactions on Communications. This is the author's version which has not been fully edited and content may change prior to final publication. Citation information: DOI 10.1109/TCOMM.2022.3199489

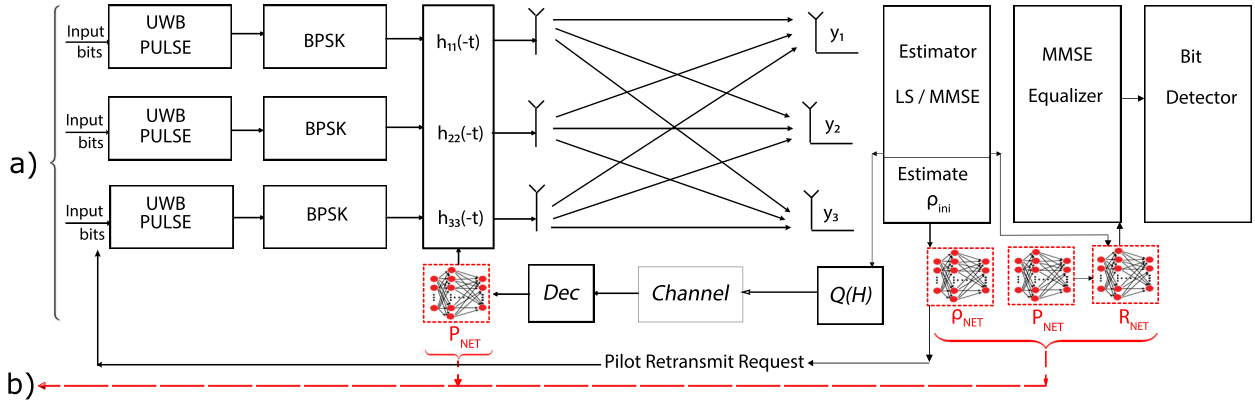

Fig. 1. (a): Conventional TR-UWB MIMO system model with explicit feedback where $Q(H)$ represents channel quantization and Dec denotes decoding with no delay; and (b): $PR\rho$-net scheme, where deep neural networks are shown in red boxes. ρ-net represents a DNN that aids the estimator in keeping track of the channel's correlation and requests pilot re-transmissions while P_{NET} and $P_{NET} - R_{NET}$ improve CSI accuracy at transmitter and equalizer, respectively.

before modulation i.e., $\mathrm{E_P} = \int_0^{T_\mathrm{P}} \mathbf{p}^2(t)dt = 1$. The measured channels utilized in the model can be expressed using a tapped delay-line model with L taps as follows

$$\mathbf{h}(t) = \sum_{l=0}^{L-1} \alpha_l \delta(t - \tau_l) \tag{2}$$

where α_l is the channel gain due to l-th ray within the cluster, τ_l represent the corresponding delay, and $\delta(t)$ is the unit-impulse function. Moreover, a block fading channel is assumed and the time variation of each channel block is governed by first order auto-regressive model [10]

$$\mathbf{h}(t) = \rho \mathbf{h}(t-1) + \sqrt{1-\rho^2}\mathbf{v} = \rho \mathbf{h}(t-1) + \sigma_v \mathbf{v} \tag{3}$$

where $\mathbf{v}$ represents noise in channel due to delay and approximated as $\mathbf{v} \backsim \mathcal{CN}(0,1)$ and $\sigma_v = \sqrt{1-\rho^2}$ governs the channel variation rate.

B. Perfect CSI Case

We consider a TR-UWB MIMO system having perfect CSI available at the transmitter, all the streams are transmitted simultaneously by pre-filtering the input signal $\mathbf{s}(t)$ with time-reversed impulse response $\mathbf{h}(-t)$. To ensure zero ISI, the pulse separation is kept greater than the delay spread of the channel. The received signal $\mathbf{y}_j$ at receiver j in TR-UWB MIMO system is given by the expression

$$\mathbf{y}_j(t) = \mathbf{s}_i(t) * \mathbf{he}_{ij}(t) + \sum_{k=1;k\neq i}^{N} \mathbf{s}_k(t) * \mathbf{he}_{kj}(t) + \mathbf{n}_j(t) \tag{4}$$

where $\mathbf{s}_i(t)$ and $\mathbf{s}_k(t)$ are the transmitted signals by the i-th and k-th antennas, $*$ represents convolution operation and $\mathbf{n}_j(t)$ is Additive White Gaussian Noise (AWGN) at receiver j. Moreover, $\mathbf{he}$ represents the equivalent channel between antennas indicated by its subscripts. The equivalent channel response $\mathbf{he}(t)$ can be represented as

$$\mathbf{he}(t) = \bar{\mathbf{H}}\mathbf{h}_\mathrm{T} = \sum_{l=0}^{L-1} \alpha_l^2 \delta(t) + \sum_{l=0}^{L-1} \sum_{z=0}^{Z-1} \alpha_l \alpha_z \delta(t - (\tau_l - \tau_z)) \tag{5}$$

where

$$\bar{\mathbf{H}} = \begin{bmatrix} h[0] & 0 & \dots & 0 \\ \vdots & h[0] & \dots & 0 \\ \vdots & \vdots & \dots & 0 \\ h[(L-1)] & \vdots & \ddots & h[0] \\ 0 & h[(L-1)] & \ddots & 0 \\ \vdots & 0 & \ddots & 0 \\ & & & h[(L-1)] \end{bmatrix} \tag{6}$$

In (5), $\bar{\mathbf{H}}$ is a Toeplitz matrix of dimension $(2L-1) \times L$, $\mathbf{h}_\mathrm{T}$ is the time-reversed version of the channel of dimension $L \times 1$. It is important to note that the received signal contains the auto-correlation of the channel impulse response for the intended antenna and $N-1$ cross-correlations of channel impulse response due to streams generated for other antennas. The $N-1$ cross-correlations of channel impulse response entitled "Multi-Stream Interference" (MSI) in literature. The first term of the right-hand side (RHS) of (4) represents the desired signal, and the second term is interference due to streams intended for other antennas. By arranging the signal transmitted by each antenna $\mathbf{s}(t)$ in a column vector $\mathbf{x} = [\mathbf{s}_1(t) \cdots\cdots \mathbf{s}_N(t)]^\mathrm{T}$, the system model with perfect CSI can be written in matrix form as

$$\mathbf{y} = \mathbf{H}\mathbf{H}_\mathrm{T}\mathbf{x} + \mathbf{n} \tag{7}$$

where

$$\mathbf{H} = \begin{bmatrix} \bar{\mathbf{H}}_{11} & \bar{\mathbf{H}}_{12} & \dots & \bar{\mathbf{H}}_{1N} \\ \bar{\mathbf{H}}_{21} & \bar{\mathbf{H}}_{22} & \dots & \bar{\mathbf{H}}_{2N} \\ \vdots & \vdots & \ddots & \vdots \\ \bar{\mathbf{H}}_{N1} & \dots & \dots & \bar{\mathbf{H}}_{NN} \end{bmatrix} \tag{8}$$

and

$$\mathbf{H}_\mathrm{T} = \begin{bmatrix} \tilde{\mathbf{H}}_{11} & \tilde{\mathbf{H}}_{12} & \dots & \tilde{\mathbf{H}}_{1N} \\ \tilde{\mathbf{H}}_{21} & \tilde{\mathbf{H}}_{22} & \dots & \tilde{\mathbf{H}}_{2N} \\ \vdots & \vdots & \ddots & \vdots \\ \tilde{\mathbf{H}}_{N1} & \dots & \dots & \tilde{\mathbf{H}}_{NN} \end{bmatrix} \tag{9}$$

This article has been accepted for publication in IEEE Transactions on Communications. This is the author's version which has not been fully edited and content may change prior to final publication. Citation information: DOI 10.1109/TCOMM.2022.3199489

where

$$\tilde{\mathbf{H}} = \begin{bmatrix} h[(L-1)] & 0 & \dots & 0 \\ \vdots & h[(L-1)] & \dots & 0 \\ \vdots & \vdots & \dots & 0 \\ h[0] & \vdots & \ddots & h[(L-1)] \\ 0 & h[0] & \ddots & 0 \\ \vdots & 0 & \ddots & 0 \\ & & & h[0] \end{bmatrix} \tag{10}$$

Note that the elements of matrices $\mathbf{H}_{\mathrm{T}}$ and $\mathbf{H}$ are arranged to maintain convolution process with signal vector $\mathbf{x}$. Moreover, $\mathbf{n}$ represents the noise vector seen at all antennas approximated by $\mathcal{CN} \backsim (0, \sigma_n^2)$. We define the energy of signal $\mathbf{x}$ as $\sigma_x^2 = \mathbb{E}[\mathbf{x}\mathbf{x}^{\mathrm{H}}]$. A simplified equivalent model of (7) can be written in matrix form as

$$\mathbf{y} = \mathbf{H}_{\mathrm{eq}}\mathbf{x} + \mathbf{n} \tag{11}$$

where $\mathbf{H}_{\mathrm{eq}}$ is equivalent response of channel and time-reversal filter given by $\mathbf{H}_{\mathrm{eq}} = \mathbf{H}\mathbf{H}_{\mathrm{T}}$. One important inference that can be drawn from the MIMO channel matrix is the small contribution of the MSI term due to uncorrelated channels and that the MSI term appears as a noise-like signal for unintended users. In the TR system, each antenna receives only one dominant signal; however, multiplexing of a large number of streams can adversely affect the performance, and for this reason, equalization is required at the receiver.

C. TR-UWB MIMO with Imperfect CSI

In this subsection, a close-loop FDD system with imperfect CSI at transmitter and receiver is considered. The transmitter sends pilot symbols periodically to form an estimate of channel $\hat{\mathbf{h}}_j$ at each receiver j. All receivers quantize the estimated channel and send back the index of the quantized channel to the transmitter. A 31 bit pilot sequence in accordance with IEEE 15.4a (Wireless Medium Access Control (MAC) and Physical Layer (PHY) specifications) is utilized for the estimation of a dense multipath channel. Let the observed signal at j-th antenna be $\mathbf{y}_j = \mathbf{X}\mathbf{h}_j + \mathbf{n}_j$, where $\mathbf{X}$ is the Toeplitz matrix of pilot symbol vector. The designed system model utilizes Least Square $\widehat{\mathbf{h}}_{j_{LS}}$ channel estimate and MMSE channel estimate $\widehat{\mathbf{h}}_{j_{MMSE}}$ given by (13) and (14) respectively.

$$\widehat{\mathbf{h}}_{j_{LS}} = (\mathbf{X}^{\mathrm{H}}\mathbf{X})^{-1}\mathbf{X}^{\mathrm{H}}\mathbf{y}_j \tag{13}$$

$$\widehat{\mathbf{h}}_{j_{MMSE}} = \mathbf{R}_{\mathrm{h}}\mathbf{X}^{\mathrm{H}}\left(\mathbf{X}\mathbf{R}_{\mathrm{h}}\mathbf{X}^{\mathrm{H}} + \sigma_{nj}^2\mathbf{I}\right)^{-1}\mathbf{y}_j \tag{14}$$

where $\mathbf{R}_{\mathrm{h}}$ is the statistical channel auto-correlation matrix, σ_{nj}^2 is the variance of noise $\mathbf{n}_j$. In $PR\rho$-net model description only MMSE estimator will be elaborated in the interest of space. The error in MMSE estimator is assumed to have a Gaussian distribution in agreement with [22] i.e., $\mathbf{e}_{est} \sim \mathcal{CN}(0, \sigma_e^2)$. The error variance σ_{e}^2 is equal to mean square estimation error given by

$$\sigma_{\mathrm{e}}^2 = \mathbf{R}_{\mathrm{h}} - \mathbf{R}_{\mathrm{h}}\mathbf{X}^{\mathrm{H}}(\mathbf{X}\mathbf{R}_{\mathrm{h}}\mathbf{X}^{\mathrm{H}} + \sigma_{nj}^2\mathbf{I})^{-1}\mathbf{R}_{\mathrm{h}}. \tag{15}$$

The estimated channel is encoded by a k-dimensional vector quantizer whose codebook is generated using the Linde-Buzo-Gray (LBG) algorithm [37]. The average distortion per sample is denoted by q and given by

$$q = \frac{1}{k}\sum_{i=1}^{P}\int_{S_i} p(x)\bar{d}(x, c_i)dx \tag{16}$$

where c_i represents the index of the codebook, $p(x)$ is the probability density function of the source, S_i represent vector quantizer partition set, $\bar{d}$ is distortion measure and P is total number of partitions. The errors due to feedback channel and noise are assumed to be diminished by introducing some redundancy with Forward Error Correcting (FEC) code. The quantization distortion is assumed to be Gaussian with zero mean and σ_{q}^2 variance i.e., $q \sim \mathcal{CN}(0, \sigma_{\mathrm{q}}^2)$. The net distortion due to estimation and quantization will cause an error signal to appear in the system, which can be assumed jointly Gaussian due to the nature of quantization and channel error. The Signal to Interference & Noise Ratio (SINR) κ_j at j-th antenna given in (12) reveals that under imperfect CSI, two additional interference terms degrade the Signal to Noise Ratio (SNR) and thus severely impacts the quality of reception. The problem of minimizing the interference terms in (12) is addressed with the help of a neural net-aided design that provides a more accurate CSI to precoder and equalizer. Moreover, our work also deals with a neural net-aided technique to detect the channel variations leading to correlation-dependent transmission of the pilot sequences. Let $\mathbf{E}_{\mathrm{T}}$ be the error matrix in time-reversal pre-filter $\mathbf{H}_{\mathrm{T}}$ that appears due to estimation and quantization errors. We can express the TR filter in this case as

$$\hat{\mathbf{H}}_{\mathrm{T}} = \mathbf{H}_{\mathrm{T}} + \mathbf{E}_{\mathrm{T}}. \tag{17}$$

The received signal can be written as

$$\mathbf{y} = \hat{\mathbf{H}}_{\mathrm{eq}}\mathbf{x} + \mathbf{n} \tag{18}$$

where $\hat{\mathbf{H}}_{\mathrm{eq}} = \mathbf{H}\hat{\mathbf{H}}_{\mathrm{T}}$. The detector calculates equivalent channel response $\hat{\mathbf{H}}_{\mathrm{eqm}} = \hat{\mathbf{H}}\hat{\mathbf{H}}_{\mathrm{T}}$ for equalization based on channel information provided by estimator. The matrix $\hat{\mathbf{H}}$ is formed by utilizing estimated channel $\widehat{\mathbf{h}}_{j_{MMSE}}$ from each antenna j. The MMSE receiver in that case is given as follows

$$\mathbf{W}_{\mathrm{MMSE}} = \left(\hat{\mathbf{H}}_{\mathrm{eqm}}^{\mathrm{H}}\hat{\mathbf{H}}_{\mathrm{eqm}} + \frac{\sigma_n^2}{\sigma_x^2}\mathbf{I}_N\right)^{-1}\hat{\mathbf{H}}_{\mathrm{eqm}}^{\mathrm{H}}. \tag{19}$$

$$\kappa_j = \frac{\mathrm{E_b}[\mathbf{he}_{ij}(t)]^2}{\mathrm{E_b}[\mathbf{he}_{ij}(t)]^2(\sigma_{\mathrm{e}}^2 + \sigma_{\mathrm{q}}^2) + \mathrm{E_b}\sum_{k=1;k\neq i}^{N}[\mathbf{he}_{kj}(t)]^2 + \mathrm{E_b}\sum_{k=1;k\neq i}^{N}[\mathbf{he}_{kj}(t)]^2(\sigma_{\mathrm{e}}^2 + \sigma_{\mathrm{q}}^2) + \sigma_{nj}^2} \tag{12}$$

IV. Deep Learning Aided design

This section will discuss a deep learning-aided technique for addressing the performance degradation issues, as well as empowering our system to use correlation-dependent transmission of the pilot sequence so as to transmit more user data instead of pilots.

A. Neural Network Augmented System

The previous section's discussion highlights that TR-UWB MIMO system performance suffers from channel imperfections at the precoder and equalizer. This deterioration in precoder and equalizer calls for a compensator to improve the SNR. The proposed novel deep learning framework that serves the mentioned purpose is shown in Fig. 1(b). This design is comprised of three fully connected (FC) neural networks, the first at the precoder denoted by $\mathrm{P_{NET}}$, the second at the receiver denoted by $\mathrm{R_{NET}}$, and the last one connected to the correlation estimator denoted by ρ_{NET}. These three neural networks are collectively dubbed $PR\rho$-net. The neural network at the precoder, i.e., $\mathrm{P_{NET}}$, is added to achieve better CSI quality, whereas $\mathrm{R_{NET}}$ at the receiver provides a more accurate equivalent channel estimate for equalization. Please note that the pre-trained $\mathrm{P_{NET}}$ is plugged as input to $\mathrm{R_{NET}}$ to aid in estimating the equivalent channel. The ρ_{NET} serves to counter noise in estimating the channel correlation ρ from data symbols that appeared in the system due to channel variation. The neural networks augmented to the system employ feed-forward fully connected design with L layers, including one input layer, $L-2$ hidden layers, and one output layer. The Rectified Linear Unit (ReLU) given by function $f_r(x) = max\{0, x\}$ is utilized as the activation function. Moreover, for each data sample v where $v = 1, 2...V$, the standard mean square error is taken as the loss function and given by

$$MSE = \frac{1}{V}\sum_{v=1}^{V}[O(v) - I(v))]^2 \tag{20}$$

where $O(v)$ and $I(v)$ represent the output and input values of training datasets, respectively. The output and input to the neural networks are depicted in Fig. 2. The offline training of P-net, R-net, and ρ-net are shown in black lines, while the red dotted lines represent online mode. These neural nets are first trained with simulated data in an offline manner, and then these neural networks can be utilized to improve the precoder, equalizer, and correlation estimator. The quantized channels and estimated equivalent channels act as input at the precoder and receiver, whereas the output is a perfect CSI dataset for training. The ρ-net is trained to provide a mapping between initially estimated parameter ρ_{ini} and actual channel correlation ρ. In all cases, the perfect CSI indicates the actually measured channels that are utilized as ground truth. Assuming the residual error, $\mathbf{E}_{\mathrm{P}}$ in precoder matrix $\hat{\mathbf{H}}_{\mathrm{P}}$, the new precoder matrix can be modeled as

$$\hat{\mathbf{H}}_{\mathrm{P}} = \mathbf{H}_{\mathrm{T}} + \mathbf{E}_{\mathrm{P}} \tag{21}$$

where $\mathbf{E}_{\mathrm{P}} \sim \mathcal{CN}(0, \mathbf{C}_{\mathrm{P}})$ and $\mathbf{C}_{\mathrm{P}} = \mathbb{E}[\mathbf{E}_{\mathrm{P}}\mathbf{E}_{\mathrm{P}}^{\mathrm{H}}]$. The MMSE equalizer utilizes the updated weight matrix $W_{\mathrm{MMSE-R}}$ that

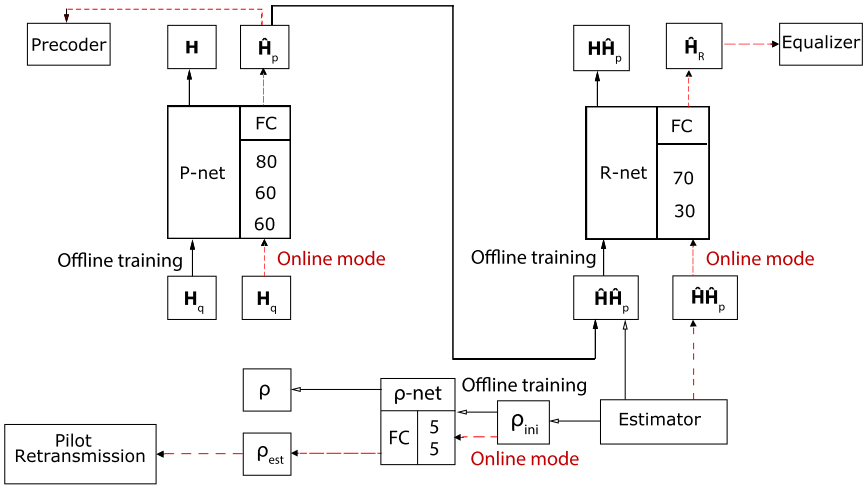

Fig. 2. PRρ-net: The input and output of PRρ-net is shown in offline (black lines) as well as online (red-dotted lines) modes. FC represents the fully-connected feed-forward neural network and number of neurons per layer are shown adjacent to it.

TABLE I
P, R AND ρ-NET DESIGN

Estimator	Neural Net	L-2	Neurons / Layer	Optimizer	MSE-Initial	MSE-Post DL
Least Square	P-Net	3	40,40,20	Adam	2.75×10^{-04}	4.30×10^{-5}
	R-Net	3	70,30,20	Levenberg-Marquardt	2.03×10^{-02}	9.60×10^{-3}
MMSE	P-Net	3	80,60,60	RMSProp	4.0×10^{-06}	3.90×10^{-07}
	R-Net	2	70,30	Levenberg-Marquardt	3.70×10^{-3}	4.62×10^{-4}
	ρ-Net	2	5,5	Levenberg-Marquardt	9.2×10^{-3}	2.30×10^{-8}

has more accurate channel information delivered to it by R-Net is given as

$$\mathbf{W}_{\mathrm{MMSE-R}} = \left(\hat{\mathbf{H}}_{\mathrm{R}}^{\mathrm{H}}\hat{\mathbf{H}}_{\mathrm{R}} + \frac{\sigma_n^2}{\sigma_x^2}\mathbf{I}_N\right)^{-1}\hat{\mathbf{H}}_{\mathrm{R}}^{\mathrm{H}} \tag{22}$$

where $\hat{\mathbf{H}}_{\mathrm{R}}$ is the output of R-net. We also assume

$$\hat{\mathbf{H}}_{\mathrm{R}} = \mathbf{H}_{\mathrm{eq}} + \mathbf{E}_{\mathrm{R}} \tag{23}$$

where $\mathbf{E}_{\mathrm{R}} \sim \mathcal{CN}(0, \mathbf{C}_{\mathrm{R}})$ and $\mathbf{C}_{\mathrm{R}} = \mathbb{E}[(\mathbf{E}_{\mathrm{R}}\mathbf{E}_{\mathrm{R}}^{\mathrm{H}}]$. The Matlab and powerful Tensorflow DNN libraries are utilized for designing neural networks. Several algorithms like Levenberg-Marquardt, Adam, and RMSProp were tested while designing the $PR\rho$-net [38]. Experiments on the small-sized networks have shown that Levenberg-Marquardt reaches a lower loss value in a similar number of iterations as Adam and RMSProp. Furthermore, the state-of-the-art optimizer like Adam has shown superiority on comparatively larger networks. Table I provides more details on the P-net, R-net, and ρ-net. We experimented with more complex and higher-dimensional deep neural networks than those shown in Table I, however, no obvious performance improvements were observed. It is important to note that P-net only serves to compensate the quantization error as the channels with the minimum mean square error are provided by the MMSE estimator.

B. Time-Varying Case

A technique to detect the channel variation in time-varying cases will be elaborated in this sub-section. In the relatively stationary environments (that are very common in cases where UWB multi-antenna systems are deployed), conventional channel estimation that relies on pilot re-transmissions can benefit from detecting channel correlation (and hence not requiring pilot re-transmissions for longer time periods), leading to more useful user data transmission in the same transmission time. Remember, the block to block channel variation is modeled using (3), now we assume that the channel varies within the same block, which causes the "outdated precoding" of the signal and thus imperfect beam-forming. The time-varying channel can be characterized by the channel correlation ρ and a random noise matrix. First we rewrite the model presented in (18) in context of $PR\rho$-net

$$\mathbf{y} = \mathbf{H}\hat{\mathbf{H}}_{\mathrm{P}}\mathbf{x} + \mathbf{n}. \tag{24}$$

The time varying channel representation of channel $\mathbf{H}$ is given by $\mathbf{H}_{\mathrm{N}}$ and can be written as

$$\mathbf{H}_{\mathrm{N}} = \rho\mathbf{H} + \sqrt{1-\rho^2}\,\mathbf{N} \tag{25}$$

where $\mathbf{N}$ is noise matrix with $\mathbf{N} \sim \mathcal{CN}(0,1)$. So (24) becomes

$$\mathbf{y} = \mathbf{H}_{\mathrm{N}}\hat{\mathbf{H}}_{\mathrm{P}}\mathbf{x} + \mathbf{n}. \tag{26}$$

Let $\hat{\mathbf{x}}$ be the detected vector at the output of MMSE equalizer given by

$$\hat{\mathbf{x}} = \mathbf{W}_{\mathrm{MMSE-R}}\mathbf{y} = (\hat{\mathbf{H}}_{\mathrm{R}}^{\mathrm{H}}\hat{\mathbf{H}}_{\mathrm{R}} + \frac{\sigma_n^2}{\sigma_x^2}\mathbf{I}_N)^{-1}\hat{\mathbf{H}}_{\mathrm{R}}^{\mathrm{H}}\mathbf{y}. \tag{27}$$

The orthogonality principal states

$$\mathbb{E}[\mathbf{e}\mathbf{y}^{\mathrm{H}}] = 0 \tag{28}$$

where error in detection $\mathbf{e} = \hat{\mathbf{x}} - \mathbf{x}$. Plugging in (26) and (27) in (28) leads to

$$\mathbb{E}\left[\mathbf{W}_{\mathrm{MMSE-R}}\right]\sigma_y^2 = \mathbb{E}[\mathbf{x}(\mathbf{H}_{\mathrm{N}}\hat{\mathbf{H}}_{\mathrm{P}}\mathbf{x} + \mathbf{n})^{\mathrm{H}}]. \tag{29}$$

Using independence between channel, input bit stream and noise i.e, $\mathbf{H}_{\mathrm{N}}\hat{\mathbf{H}}_{\mathrm{P}} \perp \mathbf{n} \perp \mathbf{x}$ also $\mathbb{E}[\mathbf{n}^{\mathrm{H}}] = 0$, $\mathbb{E}[\mathbf{x}\mathbf{x}^{\mathrm{H}}] = \sigma_x^2$, in (29) leads to

$$\mathbb{E}\left[\mathbf{W}_{\mathrm{MMSE-R}}\right]\sigma_y^2 = \sigma_x^2\,\mathbb{E}(\mathbf{H}_{\mathrm{N}}\hat{\mathbf{H}}_{\mathrm{P}})^{\mathrm{H}}. \tag{30}$$

Plugging in the value of $\mathbf{H}_{\mathrm{N}}$ and $\hat{\mathbf{H}}_{\mathrm{P}}$ from (25) and (21), further more utilizing expected value of channel $\mathbf{H}$ taken constant over a single block (block fading channel), and $\mathbb{E}[\mathbf{E}_{\mathrm{P}}] = \mathbb{E}[\mathbf{N}] = 0$, the last expression becomes

$$\mathbb{E}\left[\mathbf{W}_{\mathrm{MMSE-R}}\right]\sigma_y^2 = \sigma_x^2\left(\rho\mathbf{H}_{\mathrm{T}}^{\mathrm{H}}\mathbf{H}^{\mathrm{H}}\right). \tag{31}$$

By substituting value of $\mathbf{H}_{\mathrm{eq}}$ in (31), the new expression can be written as

$$\mathbb{E}\left[\mathbf{W}_{\mathrm{MMSE-R}}\right]\sigma_y^2 = \rho\sigma_x^2\mathbf{H}_{\mathrm{eq}}^{\mathrm{H}}. \tag{32}$$

To evaluate expected value of $\mathbf{W}_{\mathrm{MMSE-R}}$, we denote $\frac{1}{P_{\mathrm{s}}} = \frac{\sigma_n^2}{\sigma_x^2}$, where P_{s} is the SNR, so

$$\mathbb{E}\left[\mathbf{W}_{\mathrm{MMSE-R}}\right] = \mathbb{E}\left[(\hat{\mathbf{H}}_{\mathrm{R}}^{\mathrm{H}}\hat{\mathbf{H}}_{\mathrm{R}} + \frac{\mathbf{I}_N}{P_{\mathrm{s}}})^{-1}\hat{\mathbf{H}}_{\mathrm{R}}^{\mathrm{H}}\right]. \tag{33}$$

By simplifying we get

$$\mathbb{E}\left[\mathbf{W}_{\mathrm{MMSE-R}}\right] = P_{\mathrm{s}}\,\mathbb{E}\left[([\hat{\mathbf{H}}_{\mathrm{R}}^{\mathrm{H}}]^{-1} + P_{\mathrm{s}}\hat{\mathbf{H}}_{\mathrm{R}})^{-1}\right]. \tag{34}$$

Applying the Binomial Inverse Theorem [36] on R.H.S of (34) leads to

$$= P_{\mathrm{s}}\,\mathbb{E}\left[(\hat{\mathbf{H}}_{\mathrm{R}}^{\mathrm{H}} - P_{\mathrm{s}}\hat{\mathbf{H}}_{\mathrm{R}}^{\mathrm{H}}(\mathbf{I} + P_{\mathrm{s}}\hat{\mathbf{H}}_{\mathrm{R}}\hat{\mathbf{H}}_{\mathrm{R}}^{\mathrm{H}})^{-1}\hat{\mathbf{H}}_{\mathrm{R}}\hat{\mathbf{H}}_{\mathrm{R}}^{\mathrm{H}}\right]. \tag{35}$$

To simplify the inverse term we use an approximation well suited for TR-UWB MIMO systems. i.e, $(\mathbf{I}+P_{\mathrm{s}}\hat{\mathbf{H}}_{\mathrm{R}}\hat{\mathbf{H}}_{\mathrm{R}}^{\mathrm{H}}) \approx \mathbf{I}+P_{\mathrm{s}}\mathbf{I}$.

$$\mathbb{E}\left[\mathbf{W}_{\mathrm{MMSE-R}}\right] \approx P_{\mathrm{s}}\,\mathbb{E}\left[(\hat{\mathbf{H}}_{\mathrm{R}}^{\mathrm{H}} - P_{\mathrm{s}}\hat{\mathbf{H}}_{\mathrm{R}}^{\mathrm{H}}(\mathbf{I}+P_{\mathrm{s}}\mathbf{I})^{-1}\hat{\mathbf{H}}_{\mathrm{R}}\hat{\mathbf{H}}_{\mathrm{R}}^{\mathrm{H}}\right] \tag{36}$$

$$\approx P_{\mathrm{s}}\,\mathbb{E}\left[(\hat{\mathbf{H}}_{\mathrm{R}}^{\mathrm{H}} - \frac{P_{\mathrm{s}}}{(1+P_{\mathrm{s}})}\hat{\mathbf{H}}_{\mathrm{R}}^{\mathrm{H}}(\mathbf{I})^{-1}\hat{\mathbf{H}}_{\mathrm{R}}\hat{\mathbf{H}}_{\mathrm{R}}^{\mathrm{H}}\right]. \tag{37}$$

We denote the scaling factor $P_{\mathrm{n}} = \frac{P_{\mathrm{s}}}{(1+P_{\mathrm{s}})}$. Plugging in value of $\hat{\mathbf{H}}_{\mathrm{R}}$ from (23)

$$\begin{aligned}\approx P_{\mathrm{s}}\,\mathbb{E}[(\mathbf{H}_{\mathrm{eq}}^{\mathrm{H}} + \mathbf{E}_{\mathrm{R}}^{\mathrm{H}}) - P_{\mathrm{n}}[&\mathbf{H}_{\mathrm{eq}}^{\mathrm{H}}\mathbf{H}_{\mathrm{eq}}\mathbf{H}_{\mathrm{eq}}^{\mathrm{H}} + \mathbf{H}_{\mathrm{eq}}^{\mathrm{H}}\mathbf{E}_{\mathrm{R}}\mathbf{H}_{\mathrm{eq}}^{\mathrm{H}} \\ &+\mathbf{E}_{\mathrm{R}}^{\mathrm{H}}\mathbf{H}_{\mathrm{eq}}\mathbf{H}_{\mathrm{eq}}^{\mathrm{H}} + \mathbf{E}_{\mathrm{R}}^{\mathrm{H}}\mathbf{E}_{\mathrm{R}}\mathbf{H}_{\mathrm{eq}}^{\mathrm{H}} + \mathbf{H}_{\mathrm{eq}}^{\mathrm{H}}\mathbf{H}_{\mathrm{eq}}\mathbf{E}_{\mathrm{R}}^{\mathrm{H}} \\ &+\mathbf{H}_{\mathrm{eq}}^{\mathrm{H}}\mathbf{E}_{\mathrm{R}}\mathbf{E}_{\mathrm{R}}^{\mathrm{H}} + \mathbf{E}_{\mathrm{R}}^{\mathrm{H}}\mathbf{H}_{\mathrm{eq}}\mathbf{E}_{\mathrm{R}}^{\mathrm{H}} + \mathbf{E}_{\mathrm{R}}^{\mathrm{H}}\mathbf{E}_{\mathrm{R}}\mathbf{E}_{\mathrm{R}}^{\mathrm{H}}]].\end{aligned} \tag{38}$$

Utilizing $\mathbb{E}[\mathbf{E}_{\mathrm{R}}^{\mathrm{H}}] = 0$ and $\mathbb{E}[\mathbf{E}_{\mathrm{R}}\mathbf{E}_{\mathrm{R}}^{\mathrm{H}}] = \mathbf{C}_{\mathrm{R}}$, and $\mathbb{E}[\mathbf{E}_{\mathrm{R}}^{\mathrm{H}}]^2 = \mathbf{E}_{\mathrm{i}}^2$ with assumption that error matrix elements are independent of each other, $\mathbf{E}_{\mathrm{i}}^2$ is diagonal matrix with error variance at diagonal elements, furthermore by ignoring the term $\mathbf{E}_{\mathrm{R}}^{\mathrm{H}}\mathbf{E}_{\mathrm{R}}\mathbf{E}_{\mathrm{R}}^{\mathrm{H}}$ due to its very small contribution, (38) can be evaluated as

$$\begin{aligned}\mathbb{E}\left[\mathbf{W}_{\mathrm{MMSE-R}}\right] \approx P_{\mathrm{s}}\mathbf{H}_{\mathrm{eq}}^{\mathrm{H}} - P_{\mathrm{n}}[&\mathbf{H}_{\mathrm{eq}}^{\mathrm{H}}\mathbf{H}_{\mathrm{eq}}\mathbf{H}_{\mathrm{eq}}^{\mathrm{H}} + \mathbf{H}_{\mathrm{eq}}\mathbf{E}_{\mathrm{i}}^2 \\ &+2\mathbf{H}_{\mathrm{eq}}^{\mathrm{H}}\mathbf{C}_{\mathrm{R}}].\end{aligned} \tag{39}$$

By pluging (39) in (32), ρ_{ini} can be evaluated as

$$\rho_{\text{ini}} \approx [\sigma_x^2 \mathbf{H}_{\text{eq}}^{\text{H}}]^{-1}[P_{\text{s}}\mathbf{H}_{\text{eq}}^{\text{H}} - P_{\text{n}}[\mathbf{H}_{\text{eq}}^{\text{H}}\mathbf{H}_{\text{eq}}\mathbf{H}_{\text{eq}}^{\text{H}} + \mathbf{H}_{\text{eq}}\mathbf{E}_{\text{i}}^2 + 2\mathbf{H}_{\text{eq}}^{\text{H}}\mathbf{C}_{\text{R}}]]\sigma_y^2. \quad (40)$$

The above equation gives an initial estimate of channel correlation ρ_{ini}. The estimation of parameter ρ_{ini} that is derived using orthogonality condition is valid only for the MMSE case; thus, in the case of channel variation, the estimation of ρ_{ini} is affected by an addition noise. To mitigate the effect of channel variation in the estimation of ρ, we employ a neural network (ρ-net) which can map our initially estimated parameter ρ_{ini} to the actual parameter ρ. The details of the ρ-net design are furnished in Table I. The receiver's ability to detect channel variations consistently based on the received data enables it to request pilot re-transmission via feedback link when channel variation degrades the SNR beyond a certain degree. A reduction in pilot transmission can be availed so that more user data can be transmitted by implementing correlation-dependent transmission instead of regular transmission of the pilot sequence.

V. Simulation Results

The measurement of channel responses used in simulations is conducted in an indoor $14m \times 8m$ office environment. The channel frequency responses in the range of 0.7 to 6 GHz are measured using a Vector Network Analyzer (VNA) with a frequency resolution of 3.3 MHz. For the transmitter and the receiver, we use wide-band conical mono-pole antennas placed at the height of 1.5 m from the floor in a non-line of sight configuration. Using a precision positioner system, the receive antenna is moved over a rectangular surface (of dimension $65cm \times 40cm$) with a spatial resolution of 2.5cm and 5cm for the two axes of the horizontal plane. Measuring the frequency response between the transmit and receive antenna, the time-domain channel impulse response is computed using inverse Fourier transformation. More details can be found in [10]. The simulations consisted of the transmission of binary symbols over the multi-antenna system having $N = 4$ transmitter and receiver antennas. In all simulations, the estimation and quantization quality is kept fixed for a fair comparison by assuming the same SNR of 8 dB during the pilot sequence transmission, while 8 bit vector quantizer is employed to quantize the estimated channels. The ablation study of the proposed network is performed using Least Square (LS) estimator in Fig. 3. A block fading channel with $\rho = 1$ within the block is assumed in this simulation; moreover, the regular transmission of pilots after each block is considered. The bit error rate is evaluated by Montecarlo simulations using 10000 random channel realizations at each SNR. It is evident from the results that the imperfection in CSI caused by estimation and quantization errors degrades the system's performance severely. We notice that the induction of P-Net provides a limited improvement in the conventional MIMO system by reducing the error floor slightly below 10^{-2}, whereas the R-net alone performs slightly better. The combination of PR-net significantly improves the performance as it achieves a benchmark error floor of 10^{-3} at 16 dB SNR.

We compare the performance of the proposed deep learning aided $PR\rho$-net MMSE method with the state-of-the-art conventional and Deep Learning approaches in terms of BER in Fig. 4. We selected the image restoration network-based channel estimation technique elaborated in [31] for comparison as research literature is vacant concerning DL-based investigations in this domain. A block fading channel with $\rho = 1$ within the channel block and regular transmission of pilots is assumed. The proposed DL-aided $PR\rho$-net MMSE method consistently produced the lowest BER compared to all other techniques. It outperforms MMSE ordered successive interference cancellation [16] by a margin of approximately 2 dB at the SNR of 14 dB, and in comparison with Deep Learning estimation, [31], the suggested $PR\rho$-net beats the proposed image denoising technique as it only involves im-

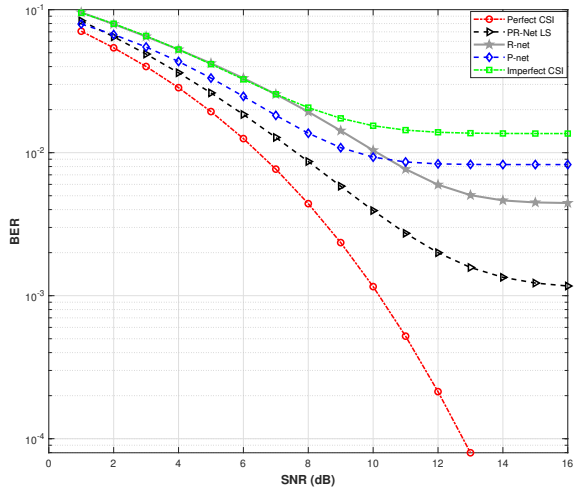

Fig. 3. $PR\rho$-net-Least square estimator

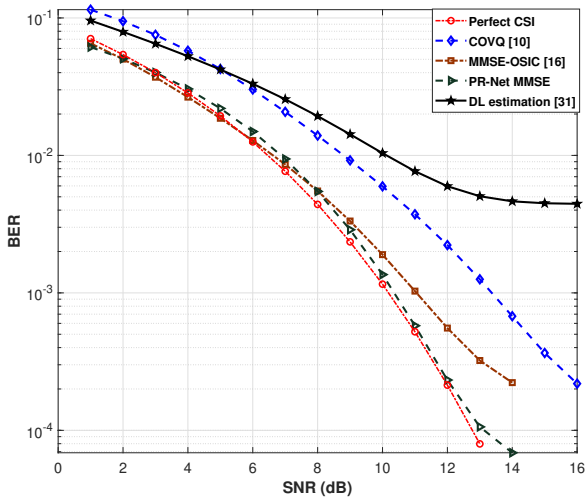

Fig. 4. $PR\rho$-net MMSE estimator comparison.

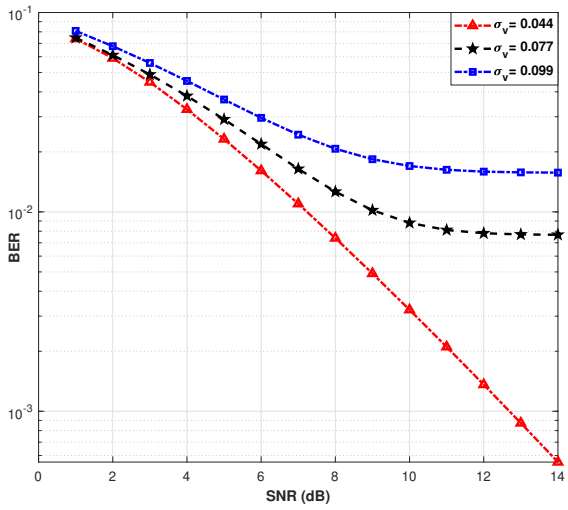

Fig. 5. σ_v effect on BER

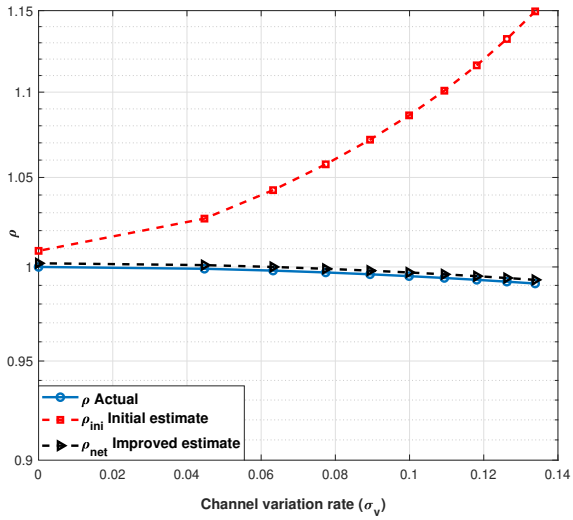

Fig. 6. Channel correlation (ρ) estimation and ρ-net compensation.

proved channel estimation at receiver. Similarly, the advantage of the proposed design is evident in comparison to COVQ [10] that only combats feedback channel noise. The results also show that we can achieve a performance close to perfect CSI by carefully designing PR-net.

To determine a suitable pilot re-transmission period, which depends upon the SNR degradation with channel variation, we assume a time-varying channel, i.e., $\rho \neq 1$ within a block, and evaluate its impact on the bit error rate in Fig. 5. The BER for different values of σ_v reveals that the variation in channel severely impacts performance. These results indicate that there is a graceful degradation in performance for $\sigma_v = 0.044$ which achieves a benchmark of 10^{-3} at 13 dB SNR approximately. For improvement in the estimation of parameter ρ_{ini} evaluated in (40), a deep neural network (ρ-net) is employed. In Fig. 6, we compare the simulation curves of actual, initial, and improved correlation values versus σ_v which represents the channel variation rate. There is an increment in estimation error of parameter ρ_{ini} as the σ_v increases because the equalizer is unaware of the channel variations. The variations in different instants of ρ_{ini} were almost negligible as the calculation of ρ_{ini} depends upon expected values. Due to the small variations, ρ-net reduced the estimation error significantly with only a few neurons. The results indicate a good agreement between the actual and improved estimates.

VI. Conclusion

In this paper, we proposed a deep learning-based novel model for precoder and equalizer error compensation in the TR-UWB MIMO system under an imperfect CSIT case. Moreover, a deep learning-aided channel tracking method and a pilot reduction strategy are also proposed. The proposed $PR\rho$-net model's bit error rate is evaluated using the Monte Carlo method utilizing multiple estimators on measured channel responses. The results suggest that the $PR\rho$-net aided system outperforms the conventional signal processing and recent DL-aided methods significantly. The proposed approach has also shown resilience in fast time-varying channel conditions as long as the channel does not decorrelate beyond a certain degree. Our analysis suggests that the proposed system with three distinct pre-trained neural networks has a lower computational load and complexity as compared to advance channel tracking algorithms; thus, it can easily be deployed to keep the legacy close-loop FDD systems alive.

References

[1] D. Tian and Q. Xiang, "Research on indoor positioning system based on UWB technology," in *Proc. 2020 IEEE 5th Information Technology and Mechatronics Engineering Conference (ITOEC)*, Chongqing, China, Jun. 2020, pp. 662–665.

[2] L. Cheng, Z. Wu, B. Lai, Q. Yang, A. Zhao, and Y. Wang, "Ultra wideband indoor positioning system based on Artificial Intelligence techniques," in *Proc. 2020 IEEE 21st International Conference on Information Reuse and Integration for Data Science (IRI)*, Las Vegas, Aug. 2020, pp. 438–444.

[3] M. Rahman, M. NagshvarianJahromi, S. S. Mirjavadi, and A. M. Hamouda, "Compact UWB band-notched antenna with integrated Bluetooth for personal wireless communication and UWB applications," *Electronics*, vol. 8, no. 2, January 2019.

[4] N. Ojaroudi Parchin, H. Jahanbakhsh Basherlou, Y. I. A. Al-Yasir, A. M. Abdulkhaleq, and R. A. Abd-Alhameed, "Ultra-wideband diversity MIMO antenna system for future mobile handsets," *Sensors*, vol. 20, no. 8, April 2020.

[5] S. Ullah, C. Ruan, M. S. Sadiq, T. U. Haq, and W. He, "High efficient and ultra wideband monopole antenna for microwave imaging and communication applications," *Sensors*, vol. 20, no. 1, December 2020.

[6] X. Yuan, W. He, K. Hong, C. Han, Z. Chen, and T. Yuan, "Ultra-wideband MIMO antenna system with high element-isolation for 5G smartphone application," *IEEE Access*, vol. 8, pp. 56 281–56 289, 2020.

[7] Y. Yang, B.-Z. Wang, and S. Ding, "Performance comparison with different antenna properties in time reversal ultra-wideband communications for sensor system applications," *Sensors*, vol. 18, no. 1, 2018.

[8] I. Naqvi and G. E. Zein, "Time reversal technique for ultra wide-band and MIMO communication systems," in *Advanced Trends in Wireless Communications*, M. Khatib, Ed. Rijeka: IntechOpen, 2011, ch. 12.

[9] R. C. Qiu, "A theory of time-reversed impulse multiple-input multiple-output (mimo) for ultra-wideband (uwb) communications," in *2006 IEEE International Conference on Ultra-Wideband*, 2006, pp. 587–592.

[10] U. Zia, M. Uppal, and I. H. Naqvi, "Robust feedback design for time reversal UWB communication systems under CSIT imperfections," *IEEE Communications Letters*, vol. 19, no. 1, pp. 102–105, Jan. 2015.

[11] T. Strohmer, M. Emami, J. Hansen, G. Papanicolaou, and A. J. Paulraj, "Application of time-reversal with MMSE equalizer to UWB communications," in *Proc. IEEE Global Telecommunications Conference*, vol. 5, Dallas TX, Nov. 2004, pp. 3123–3127.

[12] A. E. Fouda, F. L. Teixeira, and M. E. Yavuz, "Time-reversal techniques for MISO and MIMO wireless communication systems," *Radio Science*, vol. 47, no. 06, pp. 1–15, 2012.

[13] H. Nguyen, V. Nguyen, K. Nguyen, K. Maichalernnukul, F. Zheng, and T. Kaiser, "On the performance of the time reversal SM-MIMO-UWB system on correlated channels," *International Journal of Antennas and Propagation*, vol. 2012, May 2012.

[14] J. An and S. Kim, "An ordered successive interference cancellation scheme in UWB MIMO systems," *Etri Journal - ETRI J*, vol. 31, pp. 472–474, Aug. 2009.

[15] A. Zanella, M. Chiani, and M. Z. Win, "MMSE reception and successive interference cancellation for MIMO systems with high spectral efficiency," *IEEE Transactions on Wireless Communications*, vol. 4, no. 3, pp. 1244–1253, 2005.

[16] A. Iqbal, S. M. Riazul Islam, and K. S. Kwak, "Minimum mean square error-ordered successive interference cancellation (mmseosic) in uwb-mimo systems," in *2010 International Conference on Information and Communication Technology Convergence (ICTC)*, 2010, pp. 53–54.

[17] C. A. Viteri-Mera, F. L. Teixeira, and K. Sainath, "Interference-nulling time-reversal beamforming for mm-Wave massive MIMO systems," in *Proc. 2015 IEEE International Conference on Microwaves, Communications, Antennas and Electronic Systems (COMCAS)*, Tel Aviv, Israel, Nov. 2015, pp. 1–5.

[18] H. Nguyen, Z. Zhao, F. Zheng, and T. Kaiser, "Preequalizer design for spatial multiplexing SIMO-UWB TR systems," *IEEE Transactions on Vehicular Technology*, vol. 59, no. 8, pp. 3798–3805, August 2010.

[19] T. Wang and T. Lv, "Space-time pre-equalization for time reversal MIMO UWB system in strong ISI," in *Proc. 2011 IEEE International Conference on Communications (ICC)*, Kyoto, Japan, Jun. 2011, pp. 1–5.

[20] Y. Han, Y. Chen, B. Wang, and K. J. R. Liu, "Realizing massive MIMO effect using a single antenna: A time-reversal approach," in *Proc. 2016 IEEE Global Communications Conference (GLOBECOM)*, Washington DC, USA, Dec. 2016, pp. 1–6.

[21] H. Nguyen, F. Zheng, and T. Kaiser, "Antenna selection for time reversal MIMO UWB systems," in *Proc. VTC Spring 2009 - IEEE 69th Vehicular Technology Conference*, Barcelona, Spain, Apr. 2009, pp. 1–5.

[22] S. Alizadeh and H. K. Bizaki, "An enhanced MMSE based pre-processing scheme for time reversal MIMO-UWB systems in an imperfect CSI," in *Proc. 2013 21st Iranian Conference on Electrical Engineering (ICEE)*, Mashhad, Iran, May 2013, pp. 1–6.

[23] X. Liu, B. Wang, S. Xiao, and S. Lai, "Post-time-reversed MIMO ultrawideband transmission scheme," *IEEE Transactions on Antennas and Propagation*, vol. 58, no. 5, pp. 1731–1738, 2010.

[24] U. Zia, I. H. Naqvi, and M. Uppal, "Performance of ultra-wideband time-reversal systems under imperfect channel side information at the transmitter," *Electronics Letters*, vol. 51, no. 7, pp. 585–586, Apr. 2015.

[25] A. Klautau, P. Batista, N. González-Prelcic, Y. Wang, and R. W. Heath, "5G MIMO data for Machine Learning: Application to beam-selection using Deep Learning," in *2018 Information Theory and Applications Workshop (ITA)*, 2018, pp. 1–9.

[26] H. Huang, J. Yang, H. Huang, Y. Song, and G. Gui, "Deep Learning for super-resolution channel estimation and DOA estimation based massive MIMO system," *IEEE Transactions on Vehicular Technology*, vol. 67, no. 9, pp. 8549–8560, 2018.

[27] C. Wen, W. Shih, and S. Jin, "Deep Learning for massive MIMO CSI feedback," *IEEE Wireless Communications Letters*, vol. 7, no. 5, pp. 748–751, 2018.

[28] Z. Lu, J. Wang, and J. Song, "Multi-resolution csi feedback with deep learning in massive mimo system," in *Proc. 2020 IEEE International Conference on Communications (ICC)*, Dublin, Ireland, Jun. 2020, pp. 1–6.

[29] H. Ye, G. Y. Li, and B. Juang, "Power of Deep Learning for channel estimation and signal detection in OFDM systems," *IEEE Wireless Communications Letters*, vol. 7, no. 1, pp. 114–117, 2018.

[30] Y. Yang, F. Gao, X. Ma, and S. Zhang, "Deep learning-based channel estimation for doubly selective fading channels," *IEEE Access*, vol. 7, pp. 36 579–36 589, 2019.

[31] M. Soltani, V. Pourahmadi, A. Mirzaei, and H. Sheikhzadeh, "Deep learning-based channel estimation," *IEEE Communications Letters*, vol. 23, no. 4, pp. 652–655, Apr. 2019.

[32] Y. Yang, F. Gao, G. Y. Li, and M. Jian, "Deep learning-based downlink channel prediction for fdd massive mimo system," *IEEE Communications Letters*, vol. 23, no. 11, pp. 1994–1998, 2019.

[33] Y. Yang, F. Gao, Z. Zhong, B. Ai, and A. Alkhateeb, "Deep transfer learning-based downlink channel prediction for fdd massive mimo systems," *IEEE Transactions on Communications*, vol. 68, no. 12, pp. 7485–7497, 2020.

[34] F. Sohrabi, K. M. Attiah, and W. Yu, "Deep learning for distributed channel feedback and multiuser precoding in fdd massive mimo," *IEEE Transactions on Wireless Communications*, vol. 20, no. 7, pp. 4044–4057, 2021.

[35] C.-J. Chun, J.-M. Kang, and I.-M. Kim, "Deep learning-based joint pilot design and channel estimation for multiuser mimo channels," *IEEE Communications Letters*, vol. 23, no. 11, pp. 1999–2003, 2019.

[36] K. B. Petersen, M. S. Pedersen *et al.*, "The matrix cookbook," p. 510, 2008.

[37] Y. Linde, A. Buzo, and R. Gray, "An algorithm for Vector Quantizer design," *IEEE Transactions on Communications*, vol. 28, no. 1, pp. 84–95, 1980.

[38] B. M. Wilamowski, "How to not get frustrated with neural networks," in *2011 IEEE International Conference on Industrial Technology*, 2011, pp. 5–11.